

Article

High-Temperature Synthesis of Metal–Matrix Composites (Ni–Ti)–TiB₂

Vladimir Promakhov, Alexey Matveev, Nikita Schulz *, Mikhail Grigoriev, Andrey Olisov, Alexander Vorozhtsov, Alexander Zhukov and Victor Klimenko

Scientific and Educational Center “Additive Technologies”, National Research Tomsk State University, Lenin Avenue, 36, 634050 Tomsk, Russia; vvpromakhov@mail.ru (V.P.); alekey.9595@mail.ru (A.M.); mvgrigoriev@yandex.ru (M.G.); kobis@bk.ru (A.O.); abv1953@mail.ru (A.V.); zhuk_77@mail.ru (A.Z.); fablab@siberia.design (V.K.)

* Correspondence: schulznikita97@gmail.com; Tel.: +7-961-890-95-03

Abstract: Currently, metal–matrix composite materials are some of the most promising types of materials, and they combine the advantages of a metal matrix and reinforcing particles/fibres. Within the framework of this article, the high-temperature synthesis of metal–matrix composite materials based on the (Ni–Ti)–TiB₂ system was studied. The selected approaches make it possible to obtain composite materials of various compositions without contamination and with a high degree of energy efficiency during production processes. Combustion processes in the samples of a 63.5 wt.% NiB + 36.5 wt.% Ti mixture and the phase composition and structure of the synthesis products were researched. It has been established that the synthesis process in the samples proceeds via the spin combustion mechanism. It has been shown that self-propagating high-temperature synthesis (SHS) powder particles have a composite structure and consist of a Ni–Ti matrix and TiB₂ reinforcement inclusions that are uniformly distributed inside it. The inclusion size lies in the range between 0.1 and 4 µm, and the average particle size is 0.57 µm. The obtained metal–matrix composite materials can be used in additive manufacturing technologies as ligatures for heat-resistant alloys, as well as for the synthesis of composites using traditional methods of powder metallurgy.

Keywords: metal–matrix composites; high-temperature synthesis; structure; phase composition



Citation: Promakhov, V.; Matveev, A.; Schulz, N.; Grigoriev, M.; Olisov, A.; Vorozhtsov, A.; Zhukov, A.; Klimenko, V. High-Temperature Synthesis of Metal–Matrix Composites (Ni–Ti)–TiB₂. *Appl. Sci.* **2021**, *11*, 2426. <https://doi.org/10.3390/app11052426>

Academic Editors: Theodore E. Matikas and Mohammadreza Jandaghi

Received: 8 January 2021
Accepted: 6 March 2021
Published: 9 March 2021

Publisher’s Note: MDPI stays neutral with regard to jurisdictional claims in published maps and institutional affiliations.



Copyright: © 2021 by the authors. Licensee MDPI, Basel, Switzerland. This article is an open access article distributed under the terms and conditions of the Creative Commons Attribution (CC BY) license (<https://creativecommons.org/licenses/by/4.0/>).

1. Introduction

Modern engineering sets forth ambitious goals for manufacturing technologies to achieve. These goals include fabricating complex-shaped components (1) with controlled (stable) parameters of material structure and properties, (2) with bionically designed elements (designed using state-of-the-art Computer-aided engineering systems (CAE)) and (3) for optimising the functional properties of constructions. This has led to the emergence of additive manufacturing technologies that are quickly evolving to meet the challenges of modern industry.

Alloys based on Ti [1,2] and Ni [3–5] are well studied, and they have proven to be a good fit for use in the fabrication of functional parts using additive manufacturing (AM) technologies. However, with the development of aerospace, automobile and ship-building industries, materials with advanced physico-mechanical characteristics are in demand.

Metal–matrix composites (MMCs) are materials that comprise a metal matrix and ceramic inclusions. With such composites, properties can be achieved that are not otherwise possible for metal alloys in that MMCs have higher operation temperatures, wear resistance, mechanical strength and hardness [6–10]. The application of metal–matrix composites in additive manufacturing is a completely new field that will allow for an advantage in the development of an entire range of properties of fabricated items.

Unfortunately, the main approaches to the production of powder systems for use in additive manufacturing are classical metallurgical processes that are related to melting the

metal and introducing ceramic inclusions into the melt. This approach has numerous problems associated with insufficient wetting of ceramic particles by liquid metal, non-uniform distribution of particles inside the metal matrix and the flotation of these particles [11–15].

Apart from traditional technologies, there are methods for the mechanical activation or mixing of traditional single-component powders. However, the use of these methods inevitably leads to the contamination of the composition and non-uniform mixing of components. It is also not possible to obtain powders whose constituent particles are already filled with a fine-grain reinforcing phase.

The remedy here is self-propagating high-temperature synthesis (SHS), which is a technology based on exothermic reactions whereby the initial reagents react. With SHS, it is possible to obtain materials of different grades: carbides, oxides, nitrides, borides, silicides, intermetallides, etc. [16,17] Currently, scientists are mainly focused on the possibility of using SHS to obtain composites [18–26]. Some works [9–14] in the literature have demonstrated successful results in the use of SHS for obtaining composite materials with intermetallic matrices filled with dispersed ceramic inclusions. In the aforementioned works [9–14], the mechanisms of the formation of composite materials in the process of synthesis were determined, as well as the dependencies of the phase composition and structure of composites (in particular, the size of ceramic inclusions) on combustion parameters, composition of the initial charge, external influences, etc. These research works prominently feature a composition based on titanium nickelide (TiNi) and titanium diboride (TiB₂, as reinforcement particles).

In the works [26,27], research was conducted whereby (Ni-Ti)-TiB₂ composites were obtained by self-propagating high-temperature synthesis from a Ni-Ti-B powder system. The initial mixture was a stoichiometric mixture of nickel, boron and titanium powders. The obtained composites consisted of a NiTi matrix and TiB₂ particles uniformly distributed in the matrix. The sizes of ceramic inclusions ranged between 1 and 8 µm, whereas the average size was 5 µm. The results showed that the use of plasma spheroidisation made (Ni-Ti)-TiB₂ particles spherical, which allowed the use of powder materials as a raw stock for additive manufacturing. It was shown that the structure of spheroidised particles inherits the structure of the initial components. The mechanical properties of the samples obtained by selective laser sintering using composite powders surpass those of the traditional counterparts of these alloys that lack reinforcement inclusions.

Results of research [28] have determined that the use of powders of different compositions in preparing the initial mixture makes it possible to significantly reduce particle size in SHS products. Therefore, we can assume that replacing the Ni-Ti-B powder mixture with a NiB-Ti system may lead to a decrease in the size of titanium diboride particles in the (Ni-Ti)-TiB₂ composite. Based on the above experiment, in the research work described in this paper, we have decided to obtain the (Ni-Ti)-TiB₂ ceramic–metal composite from a mixture of Ti and NiB rather than from pure components.

The purpose of this research is the investigation of (1) the combustion processes (high-temperature synthesis) in the samples of metal–matrix composites made of a powder mixture (63.5 wt.% NiB + 36.5 wt.% Ti) and (2) the phase composition and structure of the synthesis products.

2. Materials and Methods

The original samples were made from a mixture of powders, titanium (Ti) and nickel-boron (NiB) (Table 1).

Table 1. Initial powders.

Powder	Particle Size (µm)	Purity (Mass %)
Ti (Polema JSC)	from 0 to 100	≥99
NiB	from 0 to 100	≥99

Titanium (Ti) and nickel-boron (NiB) powders were used as the initial materials for obtaining the samples. The components were mixed in a stoichiometric ratio: 63.5 wt.% NiB + 36.5 wt.% Ti. Then the mixture that was obtained was dried in a vacuum chamber at 200 °C over a period of 3 h. Samples with a diameter of 23 mm and a mass of 25 g from the obtained mixture were compacted. The compaction pressure was 215 MPa. The obtained compacted samples were placed in an SHS reactor whose volume was 3 litres (Figure 1a). A schematic showing the placement of the samples in the reactor is provided in Figure 1b.



Figure 1. (a) Image of the constant pressure reactor, (b) a schematic of sample placement in the reactor: 1, the sample; 2, the reactor rack; 3, VR-20/5 thermocouples (\varnothing –500 μ m); 4, the igniting molybdenum spiral; and 5, the igniting layer.

The sample (1) was installed on the stand of the reactor (2), then a thermocouple (3) was introduced into the sample perpendicular to the lateral surface of the sample, approximately in the middle.

Then, the reactor was vacuumed and then filled with an inert gas (argon) until the pressure of \sim 2.5 MPa was reached. The combustion reaction was initiated using local heating of the upper surface of the sample via the molybdenum spiral through a stamped-in igniting layer [23,29]. The composition of the igniting layer was as follows: 80 wt.% Ti + 20 wt.% B. Tungsten-rhenium thermocouples were used to measure the combustion temperature. The video of the combustion process was recorded. Then the combustion products that were obtained were ground into a powder with a ball grinder and steel balls whose diameter ranged between 6 and 15 mm.

The phase composition of the synthesis products was investigated using a Shimadzu XRD-6000 diffractometer on filtered $\text{CuK}\alpha$ radiation. The phases were detected by comparing the peaks and the obtained diffractograms with the Powder Diffraction File 4 database of the International Centre for Diffraction Data (ICDD[®]). The structure of the synthesis products was investigated on a QUANTA 200 3D scanning electron microscope with focused ion beams fitted with an energy-dispersive spectrometry (EDS) X-ray detector.

3. Results and Discussion

3.1. Research into the Process of Combustion of 63.5 wt.% NiB + 36.5 wt.% Ti Powder Mixture Samples

The process of combustion taking place in the samples of a 63.5 wt.% NiB + 36.5 wt.% Ti mixture is shown in Figure 2. It is evident that the synthesis process in the samples proceeds via the spin combustion mechanism. It has been shown that on the side surface of the compacted sample, a combustion source emerges (area 1), which then travels via a spiral trajectory (area 2) and makes a single revolution on the sample's surface (area 3). As the combustion source travels, the adjacent layer of the samples is heated and a new combustion source is formed that continues moving via a spiral trajectory.

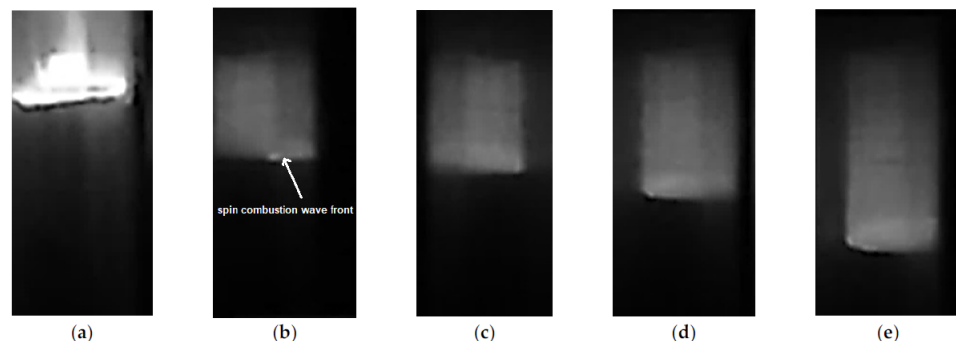


Figure 2. Images of spin combustion in the samples of the NiB-Ti mixture: (a) combustion initiation, (b) 20 s, (c) 23 s, (d) 37 s and (e) 51 s.

Spin combustion is initiated due to (1) low heat dissipation in the course of an exothermic reaction of the initial components and (2) the presence of endothermic synthesis processes in the system [1,4]. In this case, the combustion reaction is not localised in the flat layer of the sample, but rather in the zone with the largest reaction surface of the initial components. A local combustion source is formed, and it moves around the sample via a spiral trajectory.

Figure 3 shows a thermogram of combustion of the samples of the Ti-NiB powder mixture.

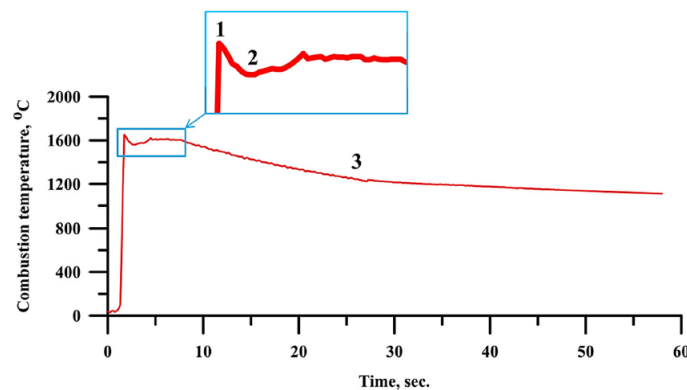


Figure 3. A thermogram of combustion of the samples of the Ti-NiB powder mixture.

The peak of the thermogram (area 1) indicates an exothermic reaction of the initial components taking place in the Ti-NiB mixture sample. The reaction is accompanied by the dissipation of a great amount of heat. The apex of the peak corresponds to the system combustion temperature, which is 1650 °C. After the peak, a small decrease in the combustion temperature is observed (area 2). This is caused by intense heat absorption in the adjacent areas of the initial mixture, which is apparently due to endothermic processes taking place in these zones. One of such processes is presumably the incongruent melting of nickel-boron. Heat absorption by the adjacent zones can be the cause of combustion front destabilisation and the formation of a spin combustion wave. Then, temperature levelling throughout the entire layer and further temperature decrease occurs, which is characteristic of the cooling of synthesis products (area 3). Here, in the time range of 8 to 27 s, the SHS materials cool more intensely compared to the time range of 27 to 78 s. This is due to the fact that impurities are emitted in the course of synthesis and they deflect the heat from the sample via convective transfer.

3.2. Investigating the Synthesis Products

The X-ray diffraction analysis of the combustion products of the Ti-NiB powder mixture has demonstrated the presence of NiTi, NiTi₂ and TiB₂ phases (Figure 4). A quantitative assessment has shown that the phases are distributed in the following proportions: 40 wt.% NiTi:6 wt.% NiTi₂:54 wt.% TiB₂.

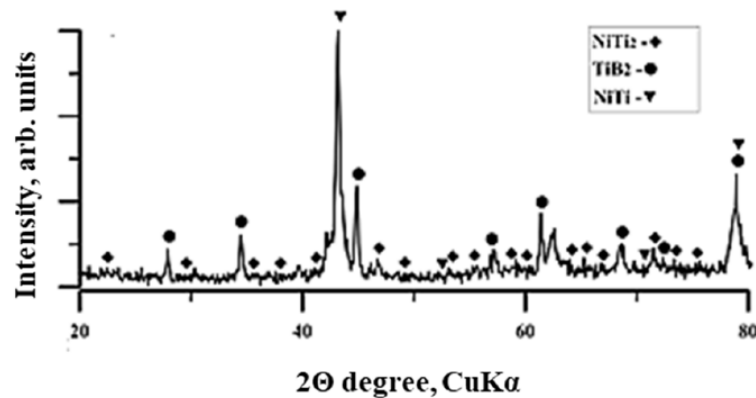


Figure 4. A typical X-ray diffraction pattern of the products of combustion of the Ti-NiB mixture.

Figure 5a,b shows SEM images of fine-ground products of combustion of the Ti-NiB mixture and the structure of the particles of the materials obtained. The results of the elementary particle analysis are shown in Figure 5c. It was determined that after fine-grinding of the products of combustion of the 63.5 wt.% NiB + 36.5 wt.% Ti system, a powder was obtained and the powder particles had an irregular sharp-corner shape. The particle size did not exceed 150 μm . It has been shown that SHS powder particles have a composite structure and consist of a matrix (area 1) and reinforcement inclusions that are uniformly distributed inside it. From the results of EDS analysis, it was determined that composite SHS powder particles contain the following elements: Ti, Ni, B, Al and Fe.

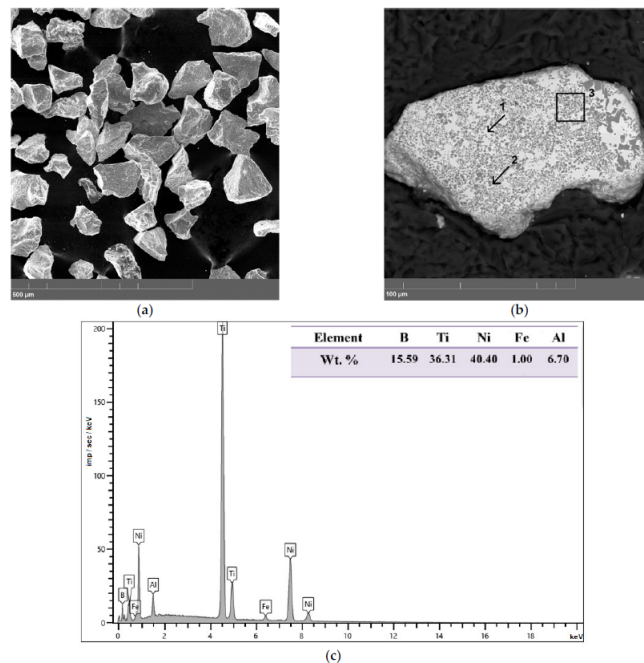


Figure 5. (a) SEM image of fine-ground products of combustion of the Ti-NiB system, (b) SEM image of the structure of the self-propagating high-temperature synthesis (SHS) powder and (c) elementary analysis of SHS powder particles.

Figure 6 shows the SEM image of a local area of a composite SHS powder particle (Figure 5, area 3). Figure 6 shows maps of the distribution of chemical elements in a local area of a composite particle. It has been proven that titanium is the main element of the composite particle and it is present in both the reinforcement inclusions and the matrix material. It has also been established that the matrix contains nickel and there are areas where aluminium elements are present. It has been found that boron is concentrated in the area of reinforcement inclusions.

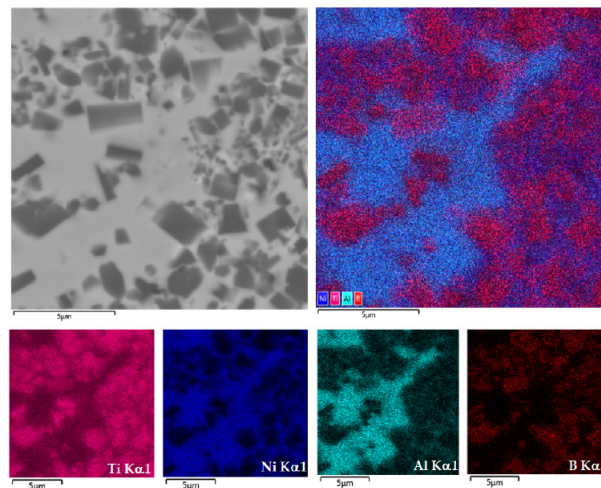


Figure 6. SEM image of a local area of a composite SHS powder particle (Figure 5, area 3) and maps of the distribution of chemical elements in a local area of a composite particle.

By comparing the results with the XRD data, it has been found that the products of combustion of the Ti-NiB powder mixture consist of an intermetallide NiTi-NiTi₂ matrix within which irregular-shaped titanium diboride (TiB₂) particles are distributed (Figure 7a). The particle size lies in the range of 0.1 to 4 μm, and the average particle size is 0.57 μm (Figure 7b). The iron in the structure of SHS powder particles was presumably scraped from the steel balls of the grinder.

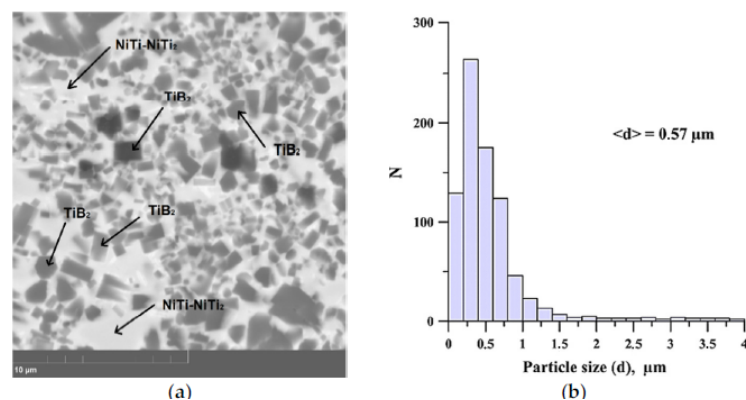


Figure 7. (a) SEM image of a local area of a composite SHS powder particle, and (b) titanium diboride particle distribution by size.

3.3. Discussion

The results obtained in the course of this investigation into the structure of composite SHS materials are in agreement with the data provided in research works [4–7,30] in the body of literature. The authors of these research works have used self-propagating high-temperature synthesis to fabricate composites where each composite comprises a matrix with ceramic particles distributed throughout its volume.

The physical and mechanical properties and features of the deformation behaviour of the obtained composite material NiTi-TiB₂ are described in article [31]. In particular, the results show that the strength properties of the TiNi matrix cannot provide the strength values that were obtained for real specimens of the cermet composite fabricated by direct laser deposition from the same powders (TiNi-TiB₂) that were synthesised by using SHS. The study of the structure of the TiNi matrix showed that the matrix material is saturated with nanosized TiB₂ particles (up to 30–40% of the volumetric content), which significantly (1.5 times) increases the mechanical characteristics of the TiNi matrices. Thus, the developed metal–ceramic composite TiNi-TiB₂ implements multilevel hardening with respect to

(1) nanosized TiB₂ particles, which are uniformly distributed over the entire metal matrix, and (2) reinforcing particles of micron size.

This work is largely devoted to the study of combustion in the SHS process and the formation of a structure in NiTi-TiB₂ particles. From the results obtained in the course of this investigation into the combustion of samples of the system consisting of 63.5 wt.% NiB + 36.5 wt.% Ti and the phase composition and structure of the combustion products, we can make suppositions about the mechanism of the formation of the NiTi-NiTi₂-TiB₂ composite. Figure 8 shows a diagram of the formation of SHS materials in the course of combustion of a Ti-NiB powder mixture in a certain local area.

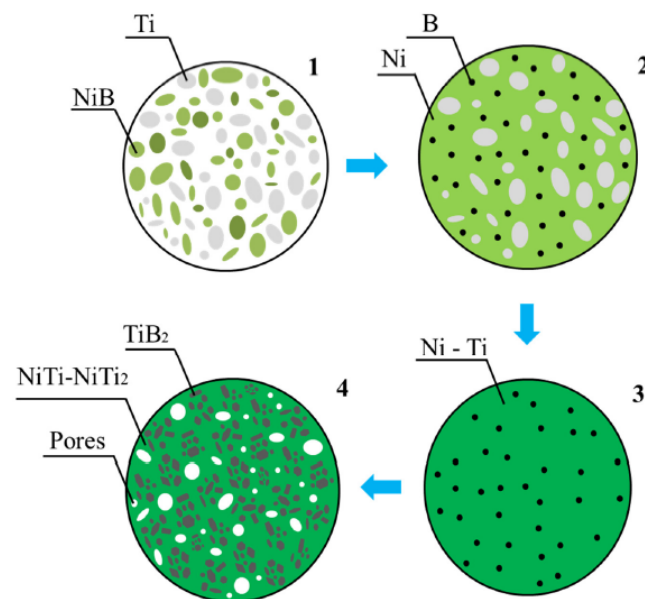


Figure 8. Schematic of the formation of the structure of the (Ni-Ti)-TiB₂ SHS composite in the course of the combustion of the Ti-NiB powder mixture.

After the top-side surface of the sample has been heated by a molybdenum spiral, the igniting layer is ignited. The dissipated heat is transferred into the main layer of the initial mixture (Figure 8, area 1) via the mechanism of conduit and convective heat transfer. A heating zone is formed, in which incongruent melting of NiB particles occurs. During melting, liquid-phase particles of nickel and boron are deposited, which are distributed in the melt together with titanium particles (Figure 8, region 2).

As shown in the Ni-Ti and Ti-B phase diagrams [9–11], titanium particles start dissolving in liquid nickel before boron particles do. A Ni-Ti melt is formed, and B particles continue dissolving in this melt (Figure 8, area 3). After the Ni-Ti melt is saturated with boron, an exothermic reaction takes place whereby titanium diboride particles are formed. At this moment, a large amount of heat is released, which is characterised by a sharp jump in temperature, with the formation of a peak in the thermogram (Figure 3, area 1). In this case, part of the heat is transferred to the next region of the sample, forming a heating zone there, and on the thermogram, this heat loss is characterised by region 2. As the synthesis products cool down, the Ni-Ti melt crystallises and NiTi and NiTi₂ phases are deposited in the process (Figure 8, area 4). These phases work as a matrix for titanium diboride particles that are distributed inside it. It can be noted that the size of the TiB₂ particles in the NiTi-TiB₂ composite obtained by SHS from the NiB-Ti powder mixture is by an order of magnitude smaller than that of the materials synthesised from the Ni-Ti-B mixture [26,27]. This confirms the hypothesis that SHS product particles decrease in size when powder compositions are used as initial mixture components, instead of powders made of pure elements. This is supposedly due to a lower synthesis temperature when incongruent melting of nickel-boron powder takes place, and the lower temperature results

in the slower growth of titanium diboride particles. In addition, boron atoms take part in the synthesis reaction and not boron particles, which results in the formation of titanium diboride particles whose size is 0.1 μm .

The data of thermogravimetric analysis and differential scanning calorimetry of the obtained materials have been studied (Figure 9). It was found that in the temperature range from 300 $^{\circ}\text{C}$ to 500 $^{\circ}\text{C}$, there is a change in the mass of the samples. Apparently, this is due to the burnout of organic substances that were added to the powders for their subsequent pressing.

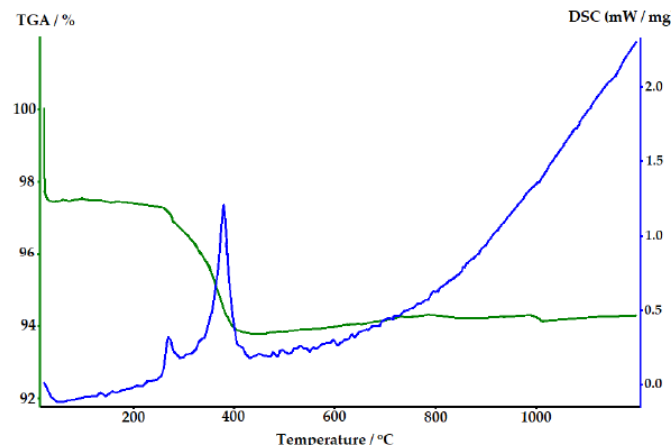


Figure 9. Results of thermogravimetric analysis and differential scanning calorimetry.

The presence of a significant amount of titanium diboride particles in the NiTi matrix most likely greatly reduces the shape memory effect, which is observed in NiTi glories. The degree of influence of the number of particles and their shape on this effect requires separate studies.

4. Conclusions

Combustion processes in the samples of a 63.5 wt.% NiB + 36.5 wt.% Ti mixture and the phase composition and structure of the synthesis products were researched.

It has been established that the synthesis process in the samples proceeds via the spin combustion mechanism. The combustion temperature in the system was 1650 $^{\circ}\text{C}$. A negligible decrease in the combustion temperature was observed, which is characteristic of the intense heat absorption that is associated with the flow of endothermic processes: incongruent melting of nickel-boron and dissolution of titanium particles in the melt.

An X-ray diffraction analysis of the combustion products of the Ti-NiB powder mixture demonstrated the presence of NiTi, NiTi₂ and TiB₂ phases. A quantitative assessment showed that the phases are distributed in the following proportions: 40 wt.% NiTi:6 wt.% NiTi₂:54 wt.% TiB₂.

After fine-grinding of the products of the 63.5 wt.% NiB + 36.5 wt.% Ti system, a powder was obtained and the powder particles had an irregular sharp-corner shape. The particle size did not exceed 150 μm . It has been shown that SHS powder particles have a composite structure and consist of a Ni-Ti matrix and TiB₂ reinforcement inclusions that are uniformly distributed inside it. The inclusion size lies in the range of 0.1 to 4 μm , and the average particle size is 0.57 μm .

Author Contributions: Conceptualisation, V.P. and A.M.; methodology, A.V.; validation, A.Z. and V.K.; formal analysis, M.G. and N.S.; investigation, A.V., N.S. and A.O.; resources, V.P.; writing—original draft preparation, V.P., A.M. and N.S.; writing—review and editing, A.Z.; visualisation, A.V.; supervision, V.P. All authors have read and agreed to the published version of the manuscript.

Funding: This research was funded by the Russian Science Foundation, grant number 20-79-10086.

Institutional Review Board Statement: Not applicable.

Informed Consent Statement: Not applicable.

Conflicts of Interest: The authors declare no conflict of interest.

References

1. Liu, G.; Chen, K.; Li, J. Combustion synthesis: An effective tool for preparing inorganic materials. *Scr. Mater.* **2018**, *157*, 167–173. [[CrossRef](#)]
2. Sun, P.; Fang, Z.; Zhang, Y.; Xia, Y. Review of the Methods for Production of Spherical Ti and Ti Alloy Powder. *JOM* **2017**, *69*, 1853–1860. [[CrossRef](#)]
3. Matveev, A.; Zhukov, I.; Ziatdinov, M.; Zhukov, A. Planetary Milling and Self-Propagating High-Temperature Synthesis of Al-TiB₂ Composites. *Materials* **2020**, *13*, 1050. [[CrossRef](#)] [[PubMed](#)]
4. Babu, S.S.; Raghavan, N.; Raplee, J.; Foster, S.J.; Frederick, C.; Haines, M.; Dinwiddie, R.; Kirka, M.K.; Plotkowski, A.; Lee, Y.; et al. Additive Manufacturing of Nickel Superalloys: Opportunities for Innovation and Challenges Related to Qualification. *Metall. Mater. Trans. A* **2018**, *49*, 3764–3780. [[CrossRef](#)]
5. Shao, S.; Khonsari, M.M.; Guo, S.; Meng, W.J.; Li, N. Overview: Additive Manufacturing Enabled Accelerated Design of Ni-based Alloys for Improved Fatigue Life. *Addit. Manuf.* **2019**, *29*, 100779. [[CrossRef](#)]
6. Fan, X.; Huang, W.; Zhou, X.; Zou, B. Preparation and characterization of NiAl-TiC-TiB₂ intermetallic matrix composite coatings by atmospheric plasma spraying of SHS powders. *Ceram. Int.* **2020**, *46*, 10512–10520. [[CrossRef](#)]
7. Imran, M.; Khan, A.R. Characterization of Al-7075 metal matrix composites: A review. *J. Mater. Res. Technol.* **2019**, *8*, 3347–3356. [[CrossRef](#)]
8. Pakash, K.S.; Gopal, P.M.; Anburose, D.; Kavimani, V. Mechanical, corrosion and wear characteristics of powder metallurgy processed Ti-6Al-4V/B₄C metal matrix composites. *Ain Shams Eng. J.* **2018**, *9*, 1489–1496.
9. Murray, J.L. Ni-Ti (Nikel-Titanium). In *Phase Diagrams of Binary Nickel Alloys*, 1st ed.; Nash, P., Ed.; ASM International: Materials Park, OH, USA, 1991; pp. 342–355.
10. Lee, K.J.; Nash, P. The Al-Ni-Ti system (Aluminum-Nickel-Titanium). *J. Phase Equilibria* **1991**, *12*, 551–562. [[CrossRef](#)]
11. Gupta, P.K.; Srivastava, R.K. Fabrication of Ceramic Reinforcement Aluminium and Its Alloys Metal Matrix Composite Materials: A Review. *Mater. Today Proc.* **2018**, *5*, 18761–18775. [[CrossRef](#)]
12. Mu, W.; Dogan, N.; Coley, K.S. In Situ Observations of Agglomeration of Non-metallic Inclusions at Steel/Ar and Steel/Slag Interfaces by High-Temperature Confocal Laser Scanning Microscope: A Review. *JOM* **2018**, *70*, 1199–1209. [[CrossRef](#)]
13. Bongaru, M.; Murugan, T.A.; Arunachalam, R. Development of Metal Matrix Nanocomposites of AA6061 SiCp Using Ultrasonic Cavitations in Squeeze Casting Process. In Proceedings of the ASME International Mechanical Engineering Congress and Exposition, Houston, TX, USA, 13–19 November 2015; p. 53151.
14. Logesh, K.; Hariharasakthisudhan, P.; Moshi, A.; Arul, M.; Rajan, B.S.; Sathickbasha, K. Mechanical properties and microstructure of A356 alloy reinforced AlN/MWCNT/graphite/Al composites fabricated by stir casting. *Mater. Res. Express* **2019**, *7*, 015004. [[CrossRef](#)]
15. Rohatgi, P.K.; Kumar, P.A.; Chellian, N.M.; Rajan, T.P.D. Solidification Processing of Cast Metal Matrix Composites Over the Last 50 Years and Opportunities for the Future. *JOM* **2020**, *72*, 2912–2926. [[CrossRef](#)]
16. Mossino, P. Some aspects in self-propagating high-temperature synthesis. *Ceram. Int.* **2004**, *30*, 311–332. [[CrossRef](#)]
17. Shekari, M.; Adeli, M.; Khobzi, A.; Kobashi, M.; Kanetake, N. Induction-activated self-propagating, high-temperature synthesis of nickel aluminide. *Adv. Powder Technol.* **2017**, *28*, 2974–2979. [[CrossRef](#)]
18. Zou, B.; Shen, P.; Jiang, Q. Reaction synthesis of TiC-TiB₂/Al composites from an Al-Ti-B₄C system. *J. Mater. Sci.* **2007**, *42*, 9927–9933. [[CrossRef](#)]
19. Liang, Y.H.; Wang, H.Y.; Yang, Y.F.; Zhao, R.Y.; Jiang, Q.C. Effect of Cu content on the reaction behaviors of self-propagating high-temperature synthesis in Cu-Ti-B₄C system. *J. Alloys Compd.* **2008**, *462*, 113–118. [[CrossRef](#)]
20. Zhang, L.; Wang, H.Y.; Li, S.T.; Liu, C.; Jiang, Q.C. Influence of reactant particle size on products of self-propagating high-temperature synthesis in 30 wt.% Cr-Ti-B₄C system. *J. Alloys Compd.* **2009**, *468*, 143–149. [[CrossRef](#)]
21. Xu, J.; Zou, B.; Tao, S.; Zhang, M.; Cao, X. Fabrication and properties of Al₂O₃-TiB₂-TiC/Al metal matrix composite coatings by atmospheric plasma spraying of SHS powders. *J. Alloys Compd.* **2016**, *672*, 251–259. [[CrossRef](#)]
22. Zou, B.; Xu, J.; Wang, Y.; Zhao, S.; Fan, X.; Hui, Y.; Zhou, X.; Huang, W.; Cai, X.; Tao, S.; et al. Self-propagating high-temperature synthesis of TiC-TiB₂-based Co cermets from a Co-Ti-B₄C system and fabrication of coatings using the cermet powders. *Chem. Eng. J.* **2013**, *223*, 138–148. [[CrossRef](#)]
23. Zhukov, I.A.; Promakhov, V.V.; Matveev, A.E.; Platov, V.V.; Khrustalev, A.P.; Dubkova, Y.A.; Vorozhtsov, S.A.; Potekaev, A.I. Principles of Structure and Phase Composition Formation in Composite Master Alloys of the Al-Ti-B/B₄C Systems Used for Aluminum Alloy Modification. *Russ. Phys. J.* **2018**, *60*, 2025–2031. [[CrossRef](#)]
24. Zhang, K.; Yin, D.; Lu, X.; Zhang, H. Self-propagating high-temperature synthesis, phase composition and aqueous durability of Nd-Al bearing zirconolite-rich composites as nuclear waste form. *Adv. Appl. Ceram.* **2018**, *117*, 78–84. [[CrossRef](#)]

25. Mazalov, A.; Shmatov, D.; Zelenina, L.; Platko, D.; Promakhov, V.; Vorozhtsov, A.; Schulz, N. Researching the Properties of Samples Fabricated Using Selective Laser Melting from A High-Temperature Nickel-Based Alloy. *Appl. Sci.* **2021**, *11*, 1419. [[CrossRef](#)]
26. Makarov, P.V.; Bakeev, R.A.; Promakhov, V.V.; Zhukov, A.S. Mechanisms of mesoscopic fracture of TiNi-TiB₂ metal-ceramic composite. *AIP Conf. Proc.* **2019**, *2167*, 020209.
27. Promakhov, V.; Zhukov, A.; Ziatdinov, M.; Zhukov, I.; Schulz, N.; Kovalchuk, S.; Dubkova, Y.; Korsmok, R.; Klimova-Korsmik, O.; Turichin, G.; et al. Inconel 625/TiB₂ Metal Matrix Composites by Direct Laser Deposition. *Metals* **2019**, *9*, 141. [[CrossRef](#)]
28. Shiganova, L.A.; Bichurov, G.V.; Amosov, A.P.; Titova, Y.V.; Ermoshkin, A.A.; Bichurova, P.G. The self-propagating high-temperature synthesis of a nanostructured titanium nitride powder with the use of sodium azide and haloid titanium-containing salt. *Russ. J. Non-Ferr. Met.* **2011**, *52*, 91–95. [[CrossRef](#)]
29. Zhukov, I.A.; Ziatdinov, M.K.; Vorozhtsov, A.B.; Zhukov, A.S.; Vorozhtsov, S.A.; Promakhov, V.V. Self-propagating high-temperature synthesis of Al and Ti borides. *Russ. Phys. J.* **2016**, *59*, 1324–1326. [[CrossRef](#)]
30. Troncy, R.; Bonnet, G.; Pedraza, F. Microstructural characterization of NiAl–Al₂O₃ composite materials obtained by in situ aluminothermic reduction of NiO for potential coating applications. *Mater. Chem. Phys.* **2020**, *251*, 123124. [[CrossRef](#)]
31. Makarov, P.V.; Bakeev, R.A.; Peryshkin, A.Y.; Zhukov, A.S.; Ziatdinov, M.K.; Promakhov, V.V. Modelling of the deformation and destruction of a TiNi-TiB₂ metal-ceramic composite fabricated by direct laser deposition. *Eng. Fract. Mech.* **2019**, *222*, 106712. [[CrossRef](#)]